



Minerva Access is the Institutional Repository of The University of Melbourne

**Author/s:**

Powell, R;Evans, KA;Green, ECR;White, RW

**Title:**

The truth and beauty of chemical potentials

**Date:**

2019-01-01

**Citation:**

Powell, R., Evans, K. A., Green, E. C. R. & White, R. W. (2019). The truth and beauty of chemical potentials. *Journal of Metamorphic Geology*, 37 (7), pp.1007-1019. <https://doi.org/10.1111/jmg.12484>.

**Persistent Link:**

<https://hdl.handle.net/11343/285832>

# Author Manuscript

This is the author manuscript accepted for publication and has undergone full peer review but has not been through the copyediting, typesetting, pagination and proofreading process, which may lead to differences between this version and the [Version of Record](#). Please cite this article as [doi: 10.1111/JMG.12484](https://doi.org/10.1111/JMG.12484)

This article is protected by copyright. All rights reserved

# 1 The truth and beauty of chemical potentials

2 R. Powell<sup>1</sup>, K.A. Evans<sup>2</sup>, E.C.R. Green<sup>3,1</sup> & R.W. White<sup>4</sup>

3 <sup>1</sup>School of Earth Sciences, University of Melbourne, Vic 3010, Australia

4 <sup>2</sup>Dept Applied Geology, Curtin University, Bentley, WA 6845, Australia

5 <sup>3</sup>Institute for Geochemistry and Petrology, ETH Zürich, Clausiusstrasse 25, CH 8092,  
6 Zürich, Switzerland,

7 <sup>4</sup>School of Earth & Environmental Sciences, University of St Andrews, KY16 9AL,  
8 Scotland, UK

9 Corresponding author: [powell@unimelb.edu.au](mailto:powell@unimelb.edu.au)

10 **Short title:** Truth and beauty of chemical potentials

## 11 Abstract

12 This essay in honour of Mike Brown addresses aspects of chemical equilibrium and  
13 equilibration in rocks, with a focus on the role that chemical potentials play. Chemical  
14 equilibrium is achieved by diffusive flattening of chemical potential gradients. The idea of  
15 equilibration volume is developed, and the way equilibration volumes may evolve along a  
16 pressure-temperature path is discussed. The effect of the environment of an equilibration  
17 volume is key to understanding the evolution of the equilibration volume with changing  
18 conditions. The likely behaviour of equilibration volumes is used to suggest why  
19 preservation of equilibrium mineral assemblages and mineral compositions from  
20 metamorphism tends to occur. This line of logic then provides the conceptual support to  
21 conventional equilibrium thermodynamic approaches to studying rocks, using, for example,  
22 thermobarometry and pseudosections.

23 **KEYWORDS** chemical potential, elastic solids; equilibration volume, equilibrium  
24 thermodynamics

# 25 1 INTRODUCTION

26 This essay on chemical potentials is in honour of Mike Brown. Amongst other things, Mike  
27 has generated and maintained the ‘space’ within geology for the ongoing development of  
28 the metamorphic geology discipline, including via this Journal. The essay follows on from  
29 Powell, Guiraud & White (2005) “Truth and beauty in metamorphic mineral equilibria:  
30 conjugate variables and phase diagrams”, in honour of D.M. Carmichael.

31 To interpret metamorphic rocks and understand metamorphic processes, a  
32 physicochemical framework is required in which to place observations on rocks. With such  
33 a framework, a view of how metamorphism occurs has been built up collectively in the  
34 metamorphic geology discipline. The view of metamorphism and metamorphic rocks  
35 adopted here, and explicitly or implicitly followed in most metamorphic papers, is outlined  
36 in detail in the Introduction and Overview sections in Powell, Evans, Green & White  
37 (2018). This paper is referred to as *nh18* below. Quoting from *nh18*: ‘Since the 1910s,  
38 with the classic work of Goldschmidt and Eskola, the striking correspondence and  
39 correlation of mineral assemblage with rock-type and orogenic “style” has been used to  
40 support the notion that the way to understand metamorphic mineral assemblages is in  
41 terms of a preserved equilibrium (e.g. Thompson, 1955; Fyfe, Turner & Verhoogen, 1958)’.  
42 And ‘The “preserved equilibrium” view of metamorphic mineral assemblages has come to  
43 form the *status quo* in metamorphic geology since that time...’. Integral to this paradigm  
44 of local equilibrium is that chemical potentials are constant over a length-scale mediated by  
45 diffusion. This paper will elaborate on the application of this view.

46 Every interpretation of mineral assemblage and mineral composition made under the  
47 thermodynamic equilibrium paradigm, including every thermodynamic calculation, makes  
48 implicit assumptions about the spatial variation of chemical potentials and the boundary  
49 conditions on the system considered. But because many of these assumptions are  
50 longstanding and little debated, the controls on chemical potential, and the features they  
51 impose on textures, are rarely discussed explicitly. This paper will elaborate on the  
52 implicit assumptions related to chemical potential and boundary conditions via a formal  
53 discussion of the central role of chemical potentials in equilibrium and equilibration in  
54 geological systems. Petrographic interpretations from the literature are reviewed in order  
55 to illustrate some common physical expressions of chemical potential behaviour.

56 What is chemical potential? For a system with multiple chemical components, the  
57 chemical potentials of these components describe the compositional dependence of the

58 relevant energy of the system. The energy then controls thermodynamic stability. A  
59 necessary condition for equilibrium is that the compositional dependence—the chemical  
60 potential—should be spatially constant. Consider temperature as an analogue for chemical  
61 potentials. In the same way that thermal equilibrium (constancy of temperature) is  
62 established by thermal equilibration involving the transfer of heat, chemical equilibrium is  
63 established by equilibration involving the transfer of matter (atoms and molecules),  
64 changing the proportions and compositions of the phases involved. As temperature is in  
65 relation to heat, so chemical potential is in relation to chemical composition. This essay  
66 begins with a formal discussion of the relationships between chemical potential, energy, and  
67 chemical composition.

## 68 **2 EQUILIBRIUM and EQUILIBRATION**

### 69 **2.1 Equilibrium**

70 Thermodynamic equilibrium is a concept that forms the cornerstone of quantitative  
71 metamorphic petrology. However, to gain insight into the thermodynamics of mineral  
72 assemblages, the physicochemical makeup of the materials involved must be simplified.  
73 Such models make the thermodynamics tractable. Results using the models then need to  
74 be assessed in the light of the differences between the predictions with the models and  
75 what is observed in real mineral assemblages. For example, an assumption that is used in  
76 the following is that grain boundaries are taken to be planar infinitely-thin interfaces  
77 between phases, that cannot hold shear-stress (they are “greased”), *nh18*, Sect. 3.1.

78 In metamorphic geology, in the greatest majority of calculations of mineral equilibria,  
79 mineral, melt and aqueous fluid phases have been treated thermodynamically as behaving  
80 in the same way mechanically, as though they are simple fluids, unable to hold shear stress.  
81 In this case the internal energy,  $U$ , of each phase is dependent on a minimal set of variables  
82 that are all scalars: entropy,  $S$ , volume,  $V$ , and composition,  $n_k$ , where  $n_k$  is the number of  
83 moles of end-member,  $k$ , e.g. Callen (1980) Sect. 1.10. The dependence of  $U$  on these  
84 variables can be formulated in terms of the intensive variables, temperature,  $\theta$ , pressure,  $p$ ,  
85 and the chemical potentials,  $\mu_k$ , respectively, e.g. Callen (1980), Sect. 2.1; Alberty (2001),  
86 Sect. 1.1; and Appendix 1.1 below. The set of pairs of conjugate variables is  $\{S, \theta\}$ ,  $\{V, p\}$   
87 and  $\{n_k, \mu_k\}$  for this model of behaviour. This model permits the use of the Gibbs energy  
88 in calculations—it is the energy that is minimised at equilibrium at constant superimposed

89 pressure and temperature, e.g. Albery (2001), Sect. 1.1; Appendix 1.1. This is then the  
90 basis of the familiar approach to rocks in which mineral equilibria are characterised by  
91 pressure and temperature and the compositions of the phases, with the compositions  
92 constant in the equilibrium.

93 In the model described above, solids at equilibrium are hydrostatically-stressed.  
94 However, it is relevant to consider the thermodynamics of solids that can be  
95 non-hydrostatically stressed at equilibrium, as undertaken in *nh18*. Any model of the solid  
96 that will allow this will need to involve a physicochemical constraint, a ‘passive resistance’  
97 of Gibbs (1906), p58. The constraint adopted in *nh18* is the one developed by Larché and  
98 Cahn (1973) called the lattice (or network) constraint (*nh18*, Sect. 3.4). Applied to an  
99 elastic solid with a crystal lattice, the lattice constraint requires that atoms and vacancies  
100 can only move by interchanges. No new lattice sites are allowed to be created or lost within  
101 a grain of solid. In other words, there is a conservation of lattice sites within the solid.  
102 Such a solid is referred to as a *lattice-constraint* solid, in contrast to an *unconstrained*  
103 phase that is not constrained in this way and can only be hydrostatically-stressed at  
104 equilibrium. For a small-strain *lattice-constraint* solid, the set of pairs of conjugate  
105 variables are  $\{S, \theta\}$ ,  $\{V_0 \mathbf{E}, \mathbf{T}\}$  and  $\{n_{k\ell}, \mu_{k\ell}\}$ , in which  $\mathbf{E}$  is the infinitesimal strain tensor  
106 and  $V_0$  is a reference volume,  $\mathbf{T}$  is the Cauchy stress tensor, and  $\mu_{k\ell}$  is the chemical  
107 potential of the exchange end-member involving the interchange of end-members  $k$  and  $\ell$   
108 (*nh18*, Sect. 3.1, 3.5; Appendix 1.1). In contrast to unconstrained solids, pressure and the  
109 chemical potentials of additive end-members do not appear in the expression for internal  
110 energy for lattice-constraint solids (*nh18*, p425). This and the consequences for equilibrium  
111 at grain boundaries are outlined in Appendix 1.3.

112 In an unconstrained phase with  $m$  independent end-members, there are  $m$  pairs in the  
113 minimal set,  $\{n_k, \mu_k\}$ . A lattice-constraint solid with  $m$  independent end-members can be  
114 represented by  $m - 1$  exchange end-members, and so involves  $m - 1$  pairs,  $\{n_{k\ell}, \mu_{k\ell}\}$ , with  
115  $k\ell$  in  $n_{k\ell}$  and  $\mu_{k\ell}$  having the meaning  $k\ell_{-1}$ . Adding a formula unit of an additive  
116 end-member to a grain increases the grain by the formula unit; adding a formula unit of an  
117 exchange end-member replaces one additive formula unit by another additive unit, leaving  
118 the number of formula units in the grain the same (*nh18*, Sect. 3.4).

119 The conventional definition of the chemical potential of any end-member,  $\ell$ , used in  
120 metamorphic geology is

$$121 \quad \mu_\ell = \left( \frac{\partial G}{\partial n_\ell} \right)_{p, T, n_{k \neq \ell}} .$$

122 This is for an unconstrained phase. In words, the chemical potential of an additive or  
123 exchange end-member is given by the rate of change of the Gibbs energy when the number  
124 of moles of the end-member is changed, while pressure, temperature and the number of  
125 moles of all other end-members is held constant. Outlined in Appendix 1.2–1.3 are other  
126 equivalent definitions for unconstrained phases and related definitions for lattice-constraint  
127 solids. A key result from Appendix 1.3 for a system involving unconstrained and  
128 lattice-constraint phases at equilibrium is that the chemical potentials of *all* end-members  
129 are defined on grain boundaries, and that these chemical potentials are all constant. For  
130 unconstrained phases—though not for lattice-constraint solids—the chemical potentials of  
131 all end-members are also defined throughout the interior of grains.

## 132 **2.2 Equilibration**

133 Features observed in rocks, such as zoned, oriented, and deformed grains, record processes  
134 that occurred during equilibration—thermal, mechanical, and chemical—as the rock  
135 adapted to changing pressures and temperatures by minimising its energy. Scalar intensive  
136 variables are constant in an equilibrium (Callen, 1985). Equilibration of scalar intensive  
137 variables involves flattening spatial gradients in those variables. A context for this is  
138 provided by classical irreversible thermodynamics (Appendix 1.5). The consequences of the  
139 flattening of gradients depend on the nature of the phases involved, and the relative rates  
140 of flattening.

141 In solids, thermal and mechanical equilibration are likely to occur faster on a given  
142 length-scale than chemical equilibration, e.g. Balluffi *at al.* (2005). For unconstrained  
143 solids, mechanical equilibrium is reached when hydrostatic pressure is attained. For  
144 lattice-constraint solids, the condition for mechanical equilibrium is that the divergence of  
145 the stress tensor is zero, which occurs when force-balance is attained for the system (*nh18*,  
146 Section 3.1). Owing to the relative rapidity of establishing thermal and mechanical  
147 equilibrium, in comparison to chemical equilibration, it is common to treat these processes  
148 as effectively instantaneous, and then consider chemical (i.e. diffusive) equilibration in  
149 solids in isolation, e.g. Larché & Cahn (1985), Sect. 7. Preservation of incomplete diffusive  
150 equilibration in rocks is considered below using this simplification.

## 151 **3** APPLYING CHEMICAL POTENTIAL IDEAS TO ROCKS

152 The results of the development above are now incorporated into discussion of chemical  
153 potentials in the context of observations in thin section of metamorphic rocks.

### 154 **3.1** Chemical potential landscapes

155 In a typical experiment on a reaction between minerals, the capsule contents are held at  
156 the experimental pressure and temperature. The starting materials are in general far from  
157 equilibrium, and equilibration occurs over the course of the experiment by evolution of the  
158 mineral assemblage. At any point in time as equilibration is underway, there is a spatial  
159 arrangement—“landscape”—of each chemical potential related to the distribution and  
160 compositions of the minerals in the experimental capsule. Each landscape flattens with  
161 time, via diffusive fluxes of the components from hills to valleys, changing the compositions  
162 and proportions of the minerals. If the experiment is continued long enough, with the  
163 pressure and temperature maintained, then equilibrium is reached when the chemical  
164 potentials flatten to become constant through the capsule. Once equilibrium is reached in  
165 the whole experimental capsule (assuming that the walls of the capsule are impermeable to  
166 all components), no further change will occur. Equilibrium thermodynamic modelling  
167 assumes that rocks have reached equilibrium in the same way that an experimental capsule  
168 does, when held at a constant pressure and temperature chosen for the experiment. But,  
169 during metamorphism, in contrast to the experimental case, rocks develop their mineral  
170 assemblages continuously with changing temperature and pressure, known as progressive  
171 metamorphism.

172 The continuously changing conditions involved in metamorphism complicate this  
173 experimental-capsule view of equilibrium. The idea of a chemical potential landscape is  
174 still useful, but such a landscape evolves with time, being dependent on temperature and  
175 pressure, even as diffusion acts to flatten relief. Moreover, unlike in an experimental  
176 capsule, there are no “walls” that constrain the part of a thin section that is being  
177 observed. The chemical potential landscapes go on, effectively, forever in space.  
178 Independent of these complexities, we can suppose *any* mineral growth or mineral  
179 composition change to be driven by the attempted flattening of chemical potential  
180 landscapes. As temperature and pressure change, the equilibrium mineral compositions  
181 change, and the discrepancy between actual and equilibrium mineral compositions induces

182 chemical potential gradients. The minerals change proportion and composition in response  
183 to these gradients in order to move towards the new equilibrium. If a new mineral  
184 nucleates, it grows if there are chemical potential gradients between it and the matrix that  
185 surrounds it that can be flattened by continued growth of the mineral.

186 To demonstrate that chemical equilibrium is broadly tracked by changing metamorphic  
187 conditions in the prograde history, at least on some length-scale, one need only invoke the  
188 very systematic metamorphic patterns that characterise orogenic belts, e.g. *nh18*, Sect 1 &  
189 2. By extension, deformation that is concomitant with metamorphism must only affect or  
190 disrupt the chemical equilibration transiently. Deformation involves textural changes in  
191 rocks that are also, at least partially, continuously overprinted. Recrystallisation, for  
192 example as a consequence of deformation, can be thought of as an equilibration process,  
193 and is probably a key one at low metamorphic temperatures and in fluid-absent systems.

### 194 **3.2 Equilibration Volume**

195 What is the length-scale of local equilibration, or, conversely, the length-scale over which  
196 chemical potential landscapes in a rock will have significant relief? Answering this question  
197 is complicated because the scale depends on which component is being considered, which  
198 solids are involved, the grain-size of the solids and so on, even without accounting for the  
199 change of temperature and pressure. With respect to any given component, complications  
200 arise as a consequence of correlated effects amongst the components.

201 For each component, for example each oxide, the term *equilibration volume* (seen by  
202 geologists as an area around a point in the context of a thin section) relates to an  
203 interpreted length-scale for equilibrium. In practice, a single equilibration volume is  
204 commonly inferred in the form of a generalised length-scale for equilibrium for a specified  
205 set of components, rather than assessing the equilibration volume for each individual  
206 component. The size of the generalised equilibration volume is most constrained by the  
207 slower diffusers in the set. Of the major elements, alumina is commonly a candidate for  
208 slowest diffuser, with, consequently, the smallest individual equilibrium volume, e.g.  
209 Carmichael (1969), but silica is an alternative in quartz-absent rocks. The length-scale of  
210 equilibration of the slowest diffuser does not preclude equilibration of faster diffusing  
211 components on a much larger scale. Equilibration volumes, while being contiguous, may  
212 contain holes, to exclude minerals or parts of minerals not in the equilibrium. In the  
213 prograde, this would include, for example, the cores of zoned porphyroblasts (see next).

214 Grain-boundary diffusion is generally likely to be faster than intragranular diffusion,  
215 particularly in fluid-bearing systems. Therefore grain size is important in considering the  
216 rate of diffusive equilibration and size of the equilibration volume. During prograde  
217 evolution, if the matrix grain size is increasing as temperature increases, then equilibration  
218 along a pressure-temperature path tends to lead to unzoned minerals, with the exception of  
219 porphyroblasts. Growth zoning of porphyroblasts occurs when growth of the grain  
220 outstrips the ability of diffusive equilibration to equilibrate the interior of the  
221 porphyroblast with the matrix, while the porphyroblast margins remain in equilibrium  
222 with adjacent matrix. Porphyroblasts will grow if the equilibrium length-scale is short  
223 compared with the characteristic distance between neighbouring porphyroblasts. The rock  
224 will contain both porphyroblast-dominated and porphyroblast-free equilibration volumes,  
225 with distinct compositions, and a transitional zone between them, across which there were  
226 chemical potential gradients. Pseudosection calculations on mineral assemblage evolution  
227 might be done using the two compositions separately. In general pseudosection calculations  
228 are inappropriate for considering the transition zone, given that it is chemical potentials  
229 not composition that control the assemblage in the transition. If, instead of two  
230 pseudosections, a whole-rock bulk composition is used, the resulting pseudosection will  
231 typically predict porphyroblasts to be consumed by subsequent reaction during further  
232 heating, even though, in the rock, the porphyroblasts appear to remain in textural  
233 equilibrium with neighbouring phases.

234 During retrograde evolution in the absence of fluid infiltration, equilibration lengths  
235 decrease as temperature decreases, while grain-sizes are, at least initially, set by processes  
236 at peak metamorphic temperatures. Decreasing equilibration length-scale as a proportion  
237 of grain size means that maintenance of equilibrium is less likely. Attempted diffusive  
238 equilibration may then lead to arrested reaction textures, including coronas.

239 In general, evolution of mineral assemblages, from the perspective of equilibration  
240 volumes, can be thought of in terms of competing effects. On the one hand, larger  
241 equilibration volumes break down to smaller ones as a consequence of changing pressure  
242 and temperature, appearance of new minerals, and so on. On the other, smaller  
243 equilibration volumes coalesce by diffusive equilibration to make larger ones. During the  
244 prograde history, the effect of increasing temperature favours the latter, whereas during the  
245 retrograde history, the former is favoured, in the absence of fluid infiltration.

246 Equilibration volume is thus quintessentially a concept related to and defined by  
247 chemical potential, though chemical potential is barely mentioned in many petrological

248 studies which nonetheless use the equilibration volume idea. Explicit consideration of  
249 chemical potential landscapes and diffusive equilibration is a powerful approach in  
250 petrographic interpretation, especially in the case of textures representing incomplete  
251 flattening of chemical potential gradients (see section 3.4, Chemical Potentials and the  
252 Rock Record below). However, such principles cannot yet be used to *predict* most textural  
253 features. Constraining the myriad physicochemical parameters needed to make such  
254 predictions lies far beyond the current scope of the discipline.

### 255 **3.3 Boundary Conditions**

256 Boundary conditions constitute another formal aspect of thermodynamics that is rarely  
257 discussed explicitly in the metamorphic petrology literature. Yet the assumed boundary  
258 conditions have a profound effect on the predicted consequences of metamorphism for rocks.

259 To explore the influence of boundary conditions, the experimental capsule analogy is  
260 continued from above, with the contents of the capsule at equilibrium, and its walls closed  
261 to diffusion. If the temperature is changed, then the consequence of this change for the  
262 contents of the capsule depends on how the wall is controlled mechanically. On the one  
263 hand, the wall may be adjusted to control the pressure it imposes on the capsule contents.  
264 On the other, the wall may be fixed, so that the capsule contents may be physically  
265 constrained (boundary condition of *place*, Truesdell & Noll, 2004, p126). For a system  
266 composed of unconstrained phases, this is equivalent to a boundary condition of constant  
267 volume. The result of equilibration in the capsule will be different in these limiting cases.  
268 The way the wall is controlled is described in terms of *boundary conditions*, the boundary  
269 being the wall of the capsule.

270 The idea of boundary conditions can be carried across to equilibration volumes in a thin  
271 section. The “boundary” in the boundary conditions of an equilibration volume is  
272 necessarily imaginary. It can be thought of as enclosing as many grains or parts of grains  
273 as constitutes the equilibration volume. The evolution of an equilibration volume depends  
274 on the boundary conditions, as in the experimental capsule analogy above. The system  
275 within the “boundary” is assumed to be at equilibrium, as constrained by the boundary  
276 conditions.

277 In the limiting case of a fixed-pressure boundary condition, the pressure within  
278 unconstrained phases at equilibrium is the same as the fixed pressure at the boundary. In  
279 the alternative limiting case of the fixed-volume boundary condition, or the boundary

280 condition of place when lattice-constraint solids are involved, the pressure in unconstrained  
281 phases takes on a constant value within the boundary. This pressure is a function of the  
282 molar volumes of the phases, and their compressibilities. In these cases, grains of  
283 lattice-constraint solids may be non-hydrostatically stressed, having pressure relations at  
284 their grain margins with unconstrained phases as outlined in Appendix 1.3. Further  
285 consideration of mechanical boundary conditions is given in Truesdell & Noll (2004).

286 Equivalent limiting cases apply to the boundary conditions relating to chemical  
287 equilibrium. The chemical potential of a component may be imposed at the boundary, and  
288 takes this value everywhere within the boundary. This requires the composition within the  
289 boundary being able to change via diffusion through the boundary. Alternatively the  
290 composition within the boundary is held constant, and the chemical potential is a  
291 consequence of the changes of phase proportions and compositions that occur there as the  
292 system comes to equilibrium at the composition specified. The first case is that of external  
293 buffering, and the second that of internal buffering. In both cases, the chemical potential  
294 within the boundary is spatially invariant at equilibrium.

295 Practical situations are likely to be intermediate between the limiting cases for both the  
296 mechanical and chemical potential boundary conditions. Consider for example the case of  
297 external buffering, with the chemical potential of a component externally-superimposed on  
298 a boundary: if the “reservoir” that the chemical potential represents is finite, then the  
299 chemical potential superimposed is likely to change with time. Further, it is rare for all  
300 intensive variables to be externally buffered. More commonly, components that diffuse  
301 easily and that partition readily into fluids are likely to be externally buffered, whereas  
302 components that are slow to diffuse and disinclined to partition into fluids are likely to be  
303 internally buffered (Korzhinskii, 1959; Evans, Powell & Frost, 2013).

304 In the conventional view of prograde metamorphic mineral assemblages, implicit in  
305 almost all mineral equilibrium calculations, a constant pressure boundary condition is  
306 adopted. This, combined with the treatment of minerals as unconstrained solids, requires  
307 that pressure is constant throughout equilibration volumes. At constant pressure, the  
308 volume change of reaction is accommodated by the environment of the equilibration  
309 volume. This accommodation may be aided by fluid escape or ingress in fluid-bearing  
310 systems, or by concomitant deformation.

311 The constant-pressure boundary condition also warrants careful consideration when  
312 retrograde reactions are considered. Rocks that have progressively lost fluid during

313 prograde metamorphism become fluid-absent near their metamorphic peak, e.g. Guiraud,  
314 Powell & Rebay (2001); White & Powell (2002), where fluids may be aqueous, carbonic or  
315 silicate. Fluid addition is then needed for reversal of prograde reactions. In fluid-absent  
316 non-deforming systems, it is harder for mineral assemblages to change volume, as they  
317 need to do for reaction to occur. The limiting mechanical boundary-condition is then one  
318 of constant volume. Furthermore, fluid-absent rocks may involve significantly slower  
319 grain-boundary diffusion than rocks with fluid. Thus, growth of new minerals and diffusive  
320 equilibration between pre-existing minerals will tend to be inhibited. The latter will  
321 include an effect known as self-stress whereby diffusion causes non-hydrostatic stress in  
322 lattice-constraint solids (e.g. Larché & Cahn, 1985, Sect. 8.3). In the absence of fluid  
323 addition, the net effect is that, with decreasing temperature in the retrograde history,  
324 equilibration volumes become progressively smaller, with mineral assemblages becoming  
325 effectively “locked” to change. These effects contribute to preservation of high grade  
326 metamorphic assemblages at the Earth’s surface (see below).

### 327 **3.4 Chemical Potentials and the Rock Record**

328 The previous sections outlined theoretical considerations related to chemical potentials,  
329 emphasizing that, within an equilibration volume, chemical potential landscapes are  
330 essentially flat—that is, chemical potentials are spatially constant. The primary record in  
331 rocks of the behaviour of chemical potentials is in the existence of recognisable  
332 equilibration volumes, via, for example, minerals having constant composition. There are,  
333 however, a number of metamorphic contexts in which *gradients* in chemical potential are  
334 preserved, having been locked into the rock before equilibration was complete. Indeed,  
335 preserved chemical potential gradients generate some of the most striking textures seen in  
336 thin section, such as coronas. They may also give valuable insight into equilibration  
337 processes that reach completion before the mineral assemblage and mineral compositions  
338 are preserved.

339 In the case of a preserved chemical potential gradient, the equilibration volume idea can  
340 be applied if, at each point in the preserved gradient, there is an (infinitely) thin  
341 equilibration volume, consistent with classical irreversible thermodynamics, e.g. Lebon *et*  
342 *al.* (2008), Ch. 2; Appendix 1.5. Moreover the chemical boundary condition of each such  
343 equilibration volume closely approaches the limiting case of external buffering, at least for  
344 faster diffusing components. Associated mineral assemblages can be predicted through

345 calculations predicated on thermodynamic equilibrium, mainly using calculated  $\mu$ - $\mu$   
346 diagrams as done in the cited papers summarised below.

347 This section describes some illustrative studies from the literature. Full details of the  
348 petrography, mineral chemistry and thermodynamic analysis of each example are given in  
349 the cited papers.

### 350 3.4.1 Chemical potential relationships during prograde metamorphism

351 During the prograde history of metamorphic rocks, diffusive equilibration is commonly  
352 effective at the thin-section length-scale, leaving scant trace of the chemical potential  
353 gradients that drove assemblage evolution. Nevertheless, evidence of equilibration and  
354 chemical potential gradients are sometimes preserved, as shown in the following examples.

355 The kyanite to sillimanite reaction on the prograde path in Barrovian metapelitic rocks  
356 is discussed in the seminal paper of Dugald Carmichael (Carmichael, 1969). The  
357 relationships are modelled in terms of calculated chemical potentials in White *et al.* (2008).  
358 Petrological observations suggest that kyanite does not break down directly to sillimanite  
359 under these conditions. In the published example, sillimanite has nucleated in biotite,  
360 rather than directly on kyanite, because the activation energy of nucleation is lower there.  
361 The presence of sillimanite sets up chemical potential gradients between parts of the rock  
362 that contain biotite+sillimanite and kyanite. From the calculations, difference in  $\mu_{K_2O}$   
363 between the parts of the rock is central, but gradients in all the chemical potentials are  
364 involved. The gradients cause the kyanite to be replaced by muscovite. If kyanite and  
365 sillimanite are still present in adjacent parts of the rock, then this most likely reflects  
366 preserved chemical potential gradients. If the kyanite is completely consumed by  
367 muscovite, the adjacent parts of the rock can form a single equilibration volume, with the  
368 chemical potential landscape flat.

369 An example of the influence of chemical potential gradients during prograde  
370 metamorphism is provided by White, Powell & Baldwin (2008), who consider the growth of  
371 a garnet porphyroblast. This is seen as a consequence of crossing a  
372  $K_2O$ - $FeO$ - $MgO$ - $Al_2O_3$ - $SiO_2$  (KFMASH) univariant reaction, with  $\mu_{FeO}$  being typically lower  
373 at the porphyroblast than in the matrix, and  $\mu_{MgO}$  being higher, driving diffusion of  $FeO$   
374 to the growing porphyroblast and  $MgO$  away from it. These chemical potential differences  
375 are maintained, with continued garnet growth, until a reactant from the univariant  
376 reaction is lost. Then the chemical potential gradients may disappear and the

377 porphyroblast stops growing. Complications induced by metamorphism along a  
378 pressure-temperature path are discussed in White *et al.* (2008).

379 An example of preserved chemical potential gradient is recorded through a prograde  
380 partial melting reaction that took place in the aluminous metapelitic rocks at Round Hill,  
381 Broken Hill (Powell & Downes, 1990; White, Powell & Halpin, 2004). In the outcrop  
382 described, leucosome occurs only around sparsely-distributed garnets. In a KFMASH system  
383 view of the reaction, the textural development can be related to the passage of the rock  
384 through the divariant fields around the biotite + sillimanite = garnet + cordierite + melt  
385 univariant (with quartz and alkali feldspar in excess), and the crossing of the univariant  
386 itself. Chemical potential gradients set up by the garnet nucleation and growth caused  
387 melt to *form* around the garnet. Melt did not form away from the garnet and percolate to  
388 its observed position. At peak conditions, chemical potential gradients can be flattened  
389 once biotite, the main reactant in the melting reaction, is consumed.

### 390 3.4.2 Chemical potential gradients during retrograde metamorphism

391 In the retrograde history of metamorphic rocks, at conditions below 700° C, retrogression  
392 tends not to produce textures related to preservation of chemical potential gradients.  
393 Addition of fluid simply causes new lower temperature mineral assemblages at the  
394 conditions of the fluid ingress. At temperature above 700° C, diffusive re-equilibration is  
395 commonly incomplete and unrelated to fluid ingress or deformation, involving anhydrous  
396 minerals and undeformed textures. Corona textures are produced when the diffusion  
397 length-scale is shorter than the pre-existing grain size for at least some of the components.  
398 A classic example, involving reaction between sapphirine and quartz, is considered in  
399 White *et al.* (2008). Monomineralic layers of sillimanite and orthopyroxene grow between  
400 the sapphirine and quartz grains, representing preserved chemical potential gradients.

401 Kyanite in felsic granulite is commonly the focus of corona textures on cooling and/or  
402 decompression. The essential structure is a zoned plagioclase moat separating the kyanite  
403 from the matrix. Also symplectitic replacements of the kyanite by spinel+plagioclase  
404 and/or sapphirine+plagioclase are commonly involved. These are modelled in Štípská,  
405 Powell, White & Baldwin (2010) and in Baldwin, Powell, White, & Štípská, (2015).  
406 Unfortunately the elegant explanation of such textures in Tajčmanová, Podlatchikov,  
407 Powell, Moulas, & Vrijmoed (2014) founders on a units problem, as discussed in *nh18*,  
408 App. 4. Various other examples involving the development of retrograde textures are

409 considered in White & Powell (2011) and Doukkari, Diener, Ouzegane & Kienast (2018).

410 The behaviour of H<sub>2</sub>O in migmatites at peak to retrograde conditions is considered in  
411 White & Powell (2010). In many migmatites the melt is physically separate from its solid  
412 residue host, as leucosomes. Chemical potential calculations show that as the melt in the  
413 leucosome/melt segregation starts to crystallise,  $\mu_{\text{H}_2\text{O}}$  in the melt segregation becomes  
414 higher than that in the host. The chemical potential gradient in H<sub>2</sub>O that this establishes  
415 causes diffusion of H<sub>2</sub>O from the leucosome into the host on a decimetre scale, where  
416 biotite grows. Crystallisation of the melt leads to anhydrous quartzo-feldspathic  
417 leucosomes, containing for example unretrogressed garnet porphyroblasts. Melt loss from  
418 leucosomes can also result in anhydrous leucosomes and the absence of garnet retrogression  
419 (Powell & Downes, 1990; White *et al.*, 2004).

### 420 3.4.3 Chemical potential gradients across lithological boundaries

421 Reaction results if chemical potential gradients are set up across the boundary between  
422 adjoining rock types. Well-documented examples involve calc-silicate layers developed  
423 between marble and pelitic schist (e.g. Brady, 1977; Joesten, 1977). For effectively-infinite  
424 marble adjoining effectively-infinite pelitic schist, the width of the calc-silicate layers is  
425 constrained only by the duration of metamorphism, as the chemical potential gradients will  
426 never be flattened. However, if the marble layers are thin and the duration of  
427 metamorphism sufficiently long, chemical potential gradients may be fully flattened, with  
428 the marble completely transformed to calc-silicate.

429 A similar example was documented by Štípská, Powell, Racek & Lexa (2014). Here,  
430 chemical potentials from a felsic granulite/melt at 12 kbar and > 900° C were superimposed  
431 on an adjacent mafic granulite derived from an eclogite in a low-strain zone at peak  
432 metamorphic conditions. The mafic granulite contains eclogitic garnet in an  
433 orthopyroxene-diopsidic clinopyroxene-plagioclase-quartz matrix derived from original  
434 omphacite. The main components involved in the transformation of this mafic granulite  
435 were H<sub>2</sub>O and K<sub>2</sub>O, the oxides predicted to be the fastest diffusers, along with Na<sub>2</sub>O.  
436 Acting on a metre scale, the chemical potentials locally transformed the mafic granulite to  
437 an intermediate composition, primarily through the growth of ternary feldspar, partly from  
438 plagioclase and partly interior to garnet. Little diffusion of Na<sub>2</sub>O occurred as  $\mu_{\text{Na}_2\text{O}}$  was  
439 similar in the felsic granulite and the mafic granulite. The transformation is inconsistent  
440 with the felsic melt infiltrating and reacting with the eclogite, because of decoupling of

441 K<sub>2</sub>O (and H<sub>2</sub>O) from other components would not occur in a simple mixture of felsic and  
442 mafic granulite. Intermediate-composition bands and bodies within related but high-strain  
443 felsic granulite may be due to such a transformation of eclogite by equilibration with the  
444 felsic granulite (Štípská *et al.*, 2014).

#### 445 3.4.4 Chemical potential gradients in reworked assemblages

446 Two final examples occur in coarse-grained plutonic igneous rocks, primarily under the  
447 influence of fluid ingress. The first is a study of the serpentinisation reactions involved in  
448 the hydration of dunite, Evans *et al.* (2013). In that study, equilibrium volumes on the  
449 scale of mm-diameter protolith grains of olivine and orthopyroxene are recognised, with  
450 assemblages varying as a function of  $\mu_{\text{SiO}_2}$ . These equilibrium volumes, or domains, are  
451 replaced by serpentine, brucite and magnetite, in the olivine domain, and by serpentine  
452 and talc in the orthopyroxene domain. The second example is provided by the textures  
453 involved in the transformation of coarse-grained plagioclase-orthopyroxene-clinopyroxene  
454 gabbro to garnet-omphacite eclogite across an apparent transformation front, Schorn &  
455 Diener (2017).

## 456 4 OUTSTANDING CONSIDERATIONS

457 One aspect of metamorphic mineral assemblage evolution that has received renewed  
458 attention recently is the idea of over-stepping of “reactions” (e.g. Spear & Pattison, 2017).  
459 In Spear & Pattison’s terminology, a reaction is the appearance of a new mineral in an  
460 assemblage represented by an appearance-of-phase line in a pseudosection. Nucleation is  
461 kinetically controlled, so its consideration in terms of an equilibrium-thermodynamic  
462 energetic displacement as in Spear & Pattison, (2017) is not appropriate; it is implicit in  
463 the development of the conceptual model described above that local equilibrium on some  
464 length-scale is maintained while nucleation and growth of new minerals occurs, regardless  
465 of any over-stepping.

466 Over-stepping may occur, in some geological situations, with energetic consequences  
467 that are significant compared with the uncertainties involved in today’s pseudosection  
468 modelling. However it is not clear currently how these energetic consequences could be  
469 estimated. Over-stepping as a consequence of homogeneous nucleation, for which good  
470 theoretical descriptions exist, is not applicable because heterogeneous nucleation is likely to

471 dominate over homogeneous nucleation on grain boundaries in metamorphic rocks, and  
472 there is little relevant theory regarding heterogeneous nucleation, Balluffi *et al.* (2005).

473 If over-stepping were common and significant, then its consequences would be different  
474 for different new minerals nucleating, and vary between rock compositions, mineral  
475 assemblage textures, etc. Thus, significant over-stepping would obscure or destroy the  
476 metamorphic patterns that are observed (e.g. *nh18*, Sect. 1). We conclude that  
477 over-stepping effects are unlikely to be commonly large in regional metamorphism.

478 The idea of the *preservation* of mineral assemblages and mineral compositions on cooling  
479 is so ubiquitous that the underlying implications are rarely considered. Yet it is unclear  
480 why preservation from metamorphism tends to correspond to local equilibrium, close to  
481 peak metamorphic conditions, and commonly on a many-grain scale, as opposed to the  
482 assemblage continuing to evolve far past peak conditions. If this preservation did not occur  
483 consistently, metamorphic patterns would be absent or obscured, and mineral equilibrium  
484 calculations would not give convincing results as commonly as they do. The intrinsic  
485 assumption, rarely articulated, is that equilibration occurs continuously along the prograde  
486 path but is then just switched off: a profound asymmetry of behaviour. A plausible  
487 explanation for the observed preservation is provided by the logic in the Boundary  
488 Conditions subsection, that a transition from a constant pressure boundary condition to a  
489 constant volume boundary condition for equilibration volumes occurs as mineral  
490 assemblages become fluid absent near the metamorphic peak, possibly also coinciding with  
491 the cessation of deformation. This is also consistent with reworking of such “locked”  
492 mineral assemblages on addition of fluid with renewed deformation. This causes reversion  
493 to constant pressure boundary conditions, dramatic increase in the size of equilibration  
494 volumes, and the appearance of new mineral assemblages that reflect local equilibrium.

#### 495 **Acknowledgements**

496 We wish to thank Simon Schorn and anonymous for their reviews, and Chris Clark for  
497 editorial handling.

498 **REFERENCES**

- 499 Alberty, R.A., 2001. Use of Legendre transforms in chemical thermodynamics. *Pure and*  
500 *Applied Chemistry* **73**, 1349–1380.
- 501 Baldwin, JA, Powell, R, White, RW, & Štípská, P. 2015. Using calculated chemical  
502 potential relationships to account for replacement of kyanite by symplectite in high  
503 pressure granulites: an example from the Snowbird tectonic zone, Canada. *Journal*  
504 *of Metamorphic Geology*, DOI:10.1111/jmg.12122.
- 505 Balluffi, R.W., Allen, S.M., & Carter, W.C., 2005. *Kinetics of Materials*. John Wiley &  
506 Sons, New York, 644pp.
- 507 Brady, J.B, 1977. Metasomatic zones in metamorphic rocks. /textitGeochemica et  
508 Cosmochemica Acta, **41**, 113–125.
- 509 Callen, H.B., 1985. *Thermodynamics and introduction to thermostatistics*. John Wiley &  
510 Sons, New York, 493pp.
- 511 Carmichael, D.M., 1969. On the mechanism of prograde metamorphic reactions in  
512 quartz-bearing pelitic rocks. *Contributions to Mineralogy and Petrology* **20**, 244–267.
- 513 Connolly, J.A.D., 2009. The geodynamic equation of state. What and how. *G-cubed*  
514 Q10014, doi:10.1029/2009GC002540.
- 515 Doukkari, S.A., Diener, J.F.A., Ouzegane, K., & Kienast, J.-R., 2018. Mineral equilibrium  
516 modelling and calculated chemical potential relations of reaction textures in the  
517 ultrahigh?temperature In Ouzzal terrane (In Hihaoua area, Western Hoggar) *Journal*  
518 *of Metamorphic Geology*, 2018; 00:1–24. <https://doi.org/10.1111/jmg.12441>.
- 519 Evans, K.A., Powell, R., & Frost, B.R., 2013. Using equilibrium thermodynamics in the  
520 study of metasomatic alteration, illustrated by an application to serpentinites.  
521 *Lithos*, **168–169**, 67–84.
- 522 Fyfe, W.S, Turner, F.J., & Verhoogen, J., 1958. *Metamorphic reactions and metamorphic*  
523 *facies*. *Geological Society of America, Memoir*, **73**, 258pp.
- 524 Gibbs, J.W., 1906. *The Scientific Papers: Thermodynamics*. Longmans, Green and co,  
525 London, 434 pp.

- 526 Guiraud, M., Powell, R., & Rebay, G., 2001. H<sub>2</sub>O in metamorphism and unexpected  
527 behaviour in the preservation of metamorphic mineral assemblages, *Journal of*  
528 *Metamorphic Geology* **19**, 445–454.
- 529 Gurtin, M.E., Fried, E. & Anand, L., 2010. *The mechanics and thermodynamics of*  
530 *continua*. Cambridge University Press, New York. 694pp.
- 531 Hillert, M., 2008. *Phase equilibria, phase diagrams, and phase transformations*.  
532 Cambridge University Press, New York. 510pp.
- 533 Joesten, R., 1977. Evolution of mineral assemblage zoning in diffusion metasomatism.  
534 *Geochimica et Cosmochimica Acta*, **47**, 283–294.
- 535 Kondepudi, D. & Prigogine, I., 1998. *Modern thermodynamics*. John Wiley & Sons,  
536 Chichester, 486pp.
- 537 Korzhinskii, D.S., 1959. *Physicochemical basis of the analysis of the paragenesis of*  
538 *minerals*, (translated from the Russian). Consultants Bureau, Inc, New York, 142pp.
- 539 Larché, F.C. & Cahn, J.W., 1973. A linear theory of thermochemical equilibrium under  
540 stress. *Acta Metallurgica* **21**, 1051–1063.
- 541 Larché, F.C. & Cahn, J.W., 1985. The interactions of composition and stress in  
542 crystalline solids. *Acta Metallurgica* **33**, 331–357.
- 543 Lebon, G., Jou, D., & Casas-Vázquez, J., 2008. *Understanding non-equilibrium*  
544 *thermodynamics*. Springer-Verlag, Heidelberg. 325pp.
- 545 Powell, R., 1978. *Equilibrium thermodynamics in petrology*. Harper & Row, London,  
546 284pp.
- 547 Powell, R., & Downes, J., 1990 Garnet porphyroblast-bearing leucosomes in metapelites:  
548 mechanisms and an example from Broken Hill, Australia, in *High temperature*  
549 *metamorphism and crustal anatexis* Ashworth, J.R., and Brown, M. (ed.) Unwin  
550 Hyman, London, pp 105–123.
- 551 Powell, R., Evans, K.A., Green, E.C.R., & White, R.W., 2018. On equilibrium in  
552 non-hydrostatic metamorphic systems. *Journal of Metamorphic Geology* **36**,  
553 419–438.

- 554 Powell, R., Holland, T.J.B., & Worley, B., 1998. Calculating phase diagrams involving  
555 solid solutions via non-linear equations, with examples using THERMOCALC  
556 *Journal of Metamorphic Geology* **16**, 577–588.
- 557 Powell, R., Guiraud, M., & White, R.W., 2005. Truth and beauty in metamorphic  
558 mineral equilibria: conjugate variables and phase diagrams. *Canadian Mineralogist*,  
559 **43**, 21–33.
- 560 Schorn, S., & Diener, J.F.A., 2017. Details of the gabbro-to-eclogite transition determined  
561 from microtextures and calculated chemical potential relationships. *Journal of*  
562 *Metamorphic Geology* **35**, 55–75.
- 563 Smith, W.R., & Missen, R.W., 1982. *Chemical reaction equilibrium analysis: theory and*  
564 *computation*. Wiley, New York, 364pp.
- 565 Spear F.S. & Pattison, D.R.M., 2017. The implications of overstepping for metamorphic  
566 assemblage diagrams (MADs). *Chemical Geology*, **457**, 38–46.
- 567 Štípská, P., Powell, R., White, R.W., & Baldwin, J.A., 2010. Using calculated chemical  
568 potential relationships to account for coronas around kyanite: an example from the  
569 Bohemian Massif. *Journal of Metamorphic Geology* **28**, 97–116.
- 570 Štípská, P., Powell, R., Racek, M., & Lexa, O. 2014. Intermediate granulite produced by  
571 transformation of eclogite at a felsic granulite contact, in Blansky les, Bohemian  
572 Massif. *Journal of Metamorphic Geology*, **32**, 347–370.
- 573 Tajčmanová, L., Podlatchikov, Y.Y., Powell, R., Moulas, E., & Vrijmoed, J.C. 2014.  
574 Grain scale pressure variations and chemical equilibrium in high-grade metamorphic  
575 rocks. *Journal of Metamorphic Geology*, **32**, 195–207.
- 576 Truesdell, C., & Noll, W., 2004. *The non-linear field theories of classical mechanics* (3ed.  
577 ed. S.S. Antman). Springer-Verlag, Heidelberg. 627pp.
- 578 Wheeler, J., 2014. Dramatic effects of stress on metamorphic reactions. *Geology*  
579 doi:10.1130/G35718.1.
- 580 White, R.W., & Powell, R., 2002. Melt loss and the preservation of granulite facies  
581 mineral assemblages. *Journal of Metamorphic Geology* **20**, 621–632.

- 582 White, R.W., Powell, R., & Halpin, J.A., 2004. Spatially-focussed melt formation in  
583 aluminous metapelites from Broken Hill, Australia: the importance of mineral  
584 texture development. *Journal of Metamorphic Geology* **22**, 825–845.
- 585 White, R.W., & Powell, R., 2010. Retrograde melt-residuum interaction and the  
586 formation of near-anhydrous leucosomes in migmatites. *Journal of Metamorphic  
587 Geology*, **28**, 579–597.
- 588 White, R.W., & Powell, R., 2011. On retrograde reaction textures in granulite facies  
589 rocks. *Journal of Metamorphic Geology*, **29**, 131–149.
- 590 White, R.W., Powell, R., & Baldwin, J.A., 2008. Calculated phase equilibria involving  
591 chemical potentials to investigate the textural evolution of metamorphic rocks.  
592 *Journal of Metamorphic Geology* **26**, 181–198.

Author Manuscript

593 **APPENDIX 1: Thermodynamic relations**

594 Some key ideas from *nh18* needed in the text are summarised here, with some additional  
 595 thermodynamics that are also needed in the text.

596 **Appendix 1.1: Variable sets and energies**

597 The fundamental relation used to express the internal energy,  $U$ , of a phase depends on  
 598 how we have chosen to model the phase, each choice having its own minimal set of  
 599 conjugate pairs of extensive and intensive variables. For the purpose of this discussion just  
 600 two behaviours—unconstrained and lattice constraint—are of interest, but in other  
 601 circumstances additional ones might be involved. In the unconstrained case, the minimal  
 602 set involves pairs of scalars,  $\{S, \theta\}$ ,  $\{V, p\}$  and  $\{n_k, \mu_k\}$ , substantially simplifying the  
 603 thermodynamic treatment. For a small-strain lattice constraint elastic solid, the minimal  
 604 set involves  $\{S, \theta\}$ ,  $\{V_0 \mathbf{E}, \mathbf{T}\}$  and  $\{n_{k\ell}, \mu_{k\ell}\}$ . The meaning of the symbols is given in the  
 605 body of the text. For the meaning and behaviour of the tensors,  $\mathbf{E}$  and  $\mathbf{T}$ , see *nh18*, Sect 3,  
 606 or the references given there, e.g., Gurtin *et al.*, (2010). For finite strain the deformation  
 607 gradient and the first Piola stress tensor can be used instead of  $\mathbf{E}$  and  $\mathbf{T}$  (e.g. Gurtin *et*  
 608 *al.*, 2010, ch. 52). Those tensors reduce to  $\mathbf{E}$  and  $\mathbf{T}$  for small strain. The presence of  
 609 tensors complicates the thermodynamic treatment. A scalar intensive variable is constant  
 610 in an equilibrium, whereas a tensor intensive variable is not constant in an equilibrium.  
 611 Instead the divergence of a tensor intensive variable is equal to zero everywhere within an  
 612 equilibrium (in the absence of an external field that affects it).

613 The fundamental relation for an unconstrained phase, representing the dependence of  $U$   
 614 on the extensive variables in the minimal set, in a variation at equilibrium, is (e.g. Callen,  
 615 1960, eq. 2.2)

$$616 \quad dU = \left( \frac{\partial U}{\partial S} \right)_{V, n_i} dS + \left( \frac{\partial U}{\partial V} \right)_{S, n_i} dV + \sum_{\ell} \left( \frac{\partial U}{\partial n_k} \right)_{V, S, n_i (i \neq k)} dn_k \quad (1)$$

617 The fundamental relation for a lattice-constraint solid is (e.g. *nh18*, eq. 7)

$$618 \quad dU = \left( \frac{\partial U}{\partial S} \right)_{\mathbf{E}, n_i} dS + \left( \frac{\partial U}{\partial \mathbf{E}} \right)_{S, n_i} : d\mathbf{E} + \sum_{k \neq \ell} \left( \frac{\partial U}{\partial n_{k\ell}} \right)_{\mathbf{E}, S, n_i (i \neq k)} dn_{k\ell} \quad (2)$$

619 Equation 2 is for a homogeneous part of the solid, allowing the strain to be represented by  
 620 a simple  $d\mathbf{E}$  term, given that strain can vary spatially within an equilibrium.

621 The derivatives in (1) and (2) can be identified with intensive variables, giving

$$622 \quad dU = \theta dS - p dV + \sum \mu_k dn_k \quad (3)$$

623 and

$$624 \quad dU = \theta dS + V_0 \mathbf{T} : d\mathbf{E} + \sum_{k \neq \ell} \mu_{k\ell} dn_{k\ell} \quad (4)$$

625 respectively, with  $V_0$  being a reference volume. The dependence of  $U$  on the extensive  
 626 variables is given in terms of the intensive variables in the corresponding conjugate pair.  
 627 The extensive variables can be thought of as natural variables.

628 The algebraic mechanism, the Legendre transform, allows the variables in a conjugate  
 629 pair in  $dU$  to be exchanged thus changing the natural variable from the extensive to the  
 630 intensive variable (Callen, 1985, p141 *et seq.*; Alberty, 2001). A Legendre transform of  $U$   
 631 with respect to  $\theta$ —transforming the thermal term—denoted  $\mathcal{L}_\theta$ , gives a new energy, the  
 632 Helmholtz energy,  $F = \mathcal{L}_\theta U$ , with  $\theta$  now the natural variable, not  $S$ . The action of the  
 633 transform on the right hand side of (3) is to replace the  $\theta dS$  term by a  $-S d\theta$  term, giving  
 634 the Helmholtz energy expression for an unconstrained phase at equilibrium

$$635 \quad dF = -S d\theta - p dV + \sum \mu_k dn_k \quad (5)$$

636 and for an homogeneous part of a lattice-constraint solid at equilibrium

$$637 \quad dF = -S d\theta + V_0 \mathbf{T} : d\mathbf{E} + \sum_{k \neq \ell} \mu_{k\ell} dn_{k\ell} \quad (6)$$

638 Transforming the thermal and mechanical terms in  $U$  gives the Gibbs energy. These  
 639 transforms have a different effect for the two behaviours being considered because the  
 640 mechanical contributions to  $U$  have a different form. The Gibbs energy for an  
 641 unconstrained phase,  $G = \mathcal{L}_{p\theta} U$ , with  $p$  and  $\theta$  now the natural variables, is

$$642 \quad dG = -S d\theta + V dp + \sum \mu_k dn_k \quad (7)$$

643 For a lattice-constraint solid,  $G = \mathcal{L}_{\mathbf{T}\theta} U$

$$644 \quad dG = -S d\theta - V_0 \mathbf{E} : d\mathbf{T} + \sum_{k \neq \ell} \mu_{k\ell} dn_{k\ell} \quad (8)$$

645 Given that Gibbs energy of a system is additive on its constituents, if all the phases in a  
 646 system are unconstrained, the Gibbs energy of the system is minimised at equilibrium, as

647 the intensive variables are all scalar and are constant through the equilibrium. This then  
 648 allows straightforward calculation of equilibrium in a system as in Connolly (2009). If any  
 649 of the phases in the system are lattice-constraint solids, their stress tensors vary spatially  
 650 in the equilibrium, so energies can no longer be minimised simply, requiring the variational  
 651 calculus as in Larché & Cahn (1973), Sect. 3b.

## 652 Appendix 1.2: Chemical potential

653 Chemical potential is defined by for an unconstrained phase by

$$654 \quad \mu_\ell = \left( \frac{\partial U}{\partial n_\ell} \right)_{S,V,n_{k \neq \ell}} = \left( \frac{\partial F}{\partial n_\ell} \right)_{\theta,V,n_{k \neq \ell}} = \left( \frac{\partial G}{\partial n_\ell} \right)_{\theta,p,n_{k \neq \ell}} \quad (9)$$

655 For a lattice-constraint solid the equivalent is

$$656 \quad \mu_{k\ell} = \left( \frac{\partial U}{\partial n_{k\ell}} \right)_{\mathbf{E},S,n_{j \neq k,\ell}} = \left( \frac{\partial F}{\partial n_{k\ell}} \right)_{\mathbf{E},\theta,n_{j \neq k,\ell}} = \left( \frac{\partial G}{\partial n_{k\ell}} \right)_{\mathbf{T},\theta,n_{j \neq k,\ell}} \quad (10)$$

657 The equivalences arise because the Legendre transforms that convert  $U$  to  $F$  and  $G$  do not  
 658 affect the chemical potential definition. In each case, the chemical potential relates to the  
 659 the way the energy changes as a consequence of a change of the number of moles of the  
 660 end-member, with the remaining natural variables in the energy held constant.

661 The chemical potential definitions in (9–10) involve the number of moles of the  
 662 end-members in the phase, whereas conceptually it is useful to think in terms of the  
 663 chemical potentials of components, e.g. oxides. The step from end-members to components  
 664 can be illustrated with nominally 1-end-member phases as explored next using the Al-Si-O  
 665 system. The key idea is that all phases are non-stoichiometric to some extent, as a  
 666 consequence of defects, primarily vacancies. The following is most easily visualised for  
 667 unconstrained phases but the conclusions are applicable more generally.

668 Chemical potentials are easier to visualise when composition is represented by mole  
 669 fraction. For unconstrained phases, Gibbs energy can be used in energy-mole fraction  
 670 diagrams, with pressure and temperature held constant. Then, on an molar Gibbs  
 671 energy-mole fraction diagram, the chemical potentials of the end-members at the  
 672 composition of a tangent to the curve for a phase are given by the values where the tangent  
 673 intersects the compositions of the end-members, e.g. Powell (1978), Ch. 2, and as  
 674 illustrated in Fig. 1. The  $G$ - $x$  loops in Fig. 1 are qualitative, and exaggerated to illustrate  
 675 that the phases are non-stoichiometric, with a range of composition across or near the

676 conventional composition for each phase. In fact, as a consequence, this conventional  
677 binary system,  $\text{Al}_2\text{O}_3\text{-SiO}_2$  should be represented in a Al-Si-O ternary system as the phases  
678 will have a range of composition that may lie off the binary line across the ternary system.  
679 Kyanite, as a nominally 1-end-member  $\text{Al}_2\text{SiO}_5$  phase, can be thought of as a model of the  
680 naturally-occurring mineral, kyanite.

681 Considering kyanite as presented in Fig. 1, if the nature and energetics of the defects in  
682 kyanite are known then the  $G$ - $x$  loop can be generated. With the  $G$ - $x$  loops, the  $\mu_{\text{SiO}_2}$  of  
683 different assemblages as a function of the  $x$  of the system are indicated adjacent to the  
684  $\text{SiO}_2$ -axis. For kyanite plus quartz or corundum,  $\mu_{\text{SiO}_2}$  (and  $\mu_{\text{Al}_2\text{O}_3}$ ) is fixed, whereas there  
685 is a range of  $\mu_{\text{SiO}_2}$  (and  $\mu_{\text{Al}_2\text{O}_3}$ ) for kyanite on its own, as its composition changes from  
686 coexistence with corundum to coexistence with quartz. It is important to realise that the  
687 values of  $\mu_{\text{SiO}_2}$  and  $\mu_{\text{Al}_2\text{O}_3}$  in kyanite are well established as a theoretical construct, even if  
688 with current knowledge they cannot be determined.

689 In Fig. 1 the range of composition of actual kyanite, or equivalently any nominally  
690 1-end-member phase, is related to how strongly-curved the  $G$ - $x$  loop is at its tip. The  $\mu_{\text{SiO}_2}$   
691 increases with  $\text{SiO}_2$  in kyanite. In the conceptual limit the  $G$ - $x$  loop can be reduced to a  
692 vertical line at the  $\text{Al}_2\text{SiO}_5$  composition. Then the essential relationships remain, but  
693 without the relationship between  $\mu$  and composition for the one-phase kyanite. The same  
694 applies to quartz and corundum if their  $G$ - $x$  loops are reduced to vertical lines at  $\text{SiO}_2$  and  
695  $\text{Al}_2\text{O}_3$  respectively. Thus, even for model 1-end-member phases,  $\mu$  of components, in this  
696 case, oxides, are defined even if the phases are idealised.

697 In a binary system, if a phase involves an energetically-favourable, typically  
698 stoichiometric substitution, such as  $\text{FeMg}_{-1}$ , then the  $G$ - $x$  loop is open and rounded, rather  
699 than strongly curved. This shape allows a wide range of possible compositions of the  
700 phase, depending on the  $G$ - $x$  loops of possible coexisting minerals. In larger systems, the  
701 multi-dimensional  $G$ - $x$  loops will be sharp in substitution directions that are energetically  
702 unfavourable, commonly non-stoichiometric, ones, but open and rounded in easy  
703 substitution directions. For example, consider plagioclase, conventionally idealised as  
704 binary anorthite-albite,  $\text{CaAl}_2\text{Si}_2\text{O}_8\text{-NaAlSi}_3\text{O}_8$ . In the system  $\text{Na}_2\text{O-CaO-Al}_2\text{O}_3\text{-SiO}_2$ , the  
705 plagioclase  $G$ - $x$  loop will be rounded and open between the albite and anorthite  
706 compositions but sharp in other dimensions.

707 The main result of this Appendix section so far is that the chemical potentials of, say,  
708 oxides, are defined in all unconstrained phases. Given the convenience, and indeed

709 practical necessity, of considering model phases, for example  $\text{Al}_2\text{SiO}_5$  for kyanite, or  
710  $\text{CaAl}_2\text{Si}_2\text{O}_8\text{-NaAlSi}_3\text{O}_8$  for plagioclase, it remains to be established how the statement of  
711 equilibrium in terms of constancy of the  $\mu$  of, say, oxides, translates to equilibrium stated  
712 in terms of the  $\mu$  of end-members of the phases in an equilibrium. With  $\mu_{\text{Al}_2\text{SiO}_5}$  fixed by  
713 the presence of model kyanite in an equilibrium, then  $\mu_{\text{Al}_2\text{SiO}_5} = \mu_{\text{Al}_2\text{O}_3} + \mu_{\text{SiO}_2}$ , just from  
714 the geometry of the  $G$ - $x$  diagram, Fig. 1, and the role of tangents to  $G$ - $x$  loops. Then,  
715 given that  $\mu_{\text{Al}_2\text{O}_3}$  and  $\mu_{\text{SiO}_2}$  are constant in an equilibrium, so is  $\mu_{\text{Al}_2\text{SiO}_5}$ . If there are other  
716 phases in equilibrium with the kyanite, the end-members of each of these phases can be  
717 written in terms of a sum of  $\mu$  of end-members, with multipliers from the number of oxides  
718 in the end-member formulae. The collected  $\mu$  equivalences can be combined to make  
719 equilibrium relations just in terms of  $\mu$  of the main end-members. A trivial example is  
720 coexisting kyanite, sillimanite and quartz giving one equilibrium relation,  
721  $\mu_{\text{Al}_2\text{SiO}_5}^{\text{ky}} = \mu_{\text{Al}_2\text{SiO}_5}^{\text{sill}}$ . In this equilibrium,  $\mu_{\text{SiO}_2}$  is specified by the presence of quartz, but  
722  $\mu_{\text{Al}_2\text{O}_3}$  is unspecified, although the fact that it is defined and constant in the equilibrium is  
723 used in generating the equilibrium relation. An alternative derivation of equilibrium  
724 relations is given in Appendix 1.4. THERMOCALC performs its calculations with an  
725 independent set of equilibrium relations between end-members of the phases in an  
726 equilibrium (Powell, Holland & Worley, 1998).

### 727 Appendix 1.3: Equilibrium within and between grains

728 Whereas the idea of pressure is firmly anchored in physics (as force acting perpendicularly  
729 on unit area), that does not mean that this quantity always plays a primary role in the  
730 thermodynamics of a phase. In *nh18*, the *thermodynamic* pressure is defined by

$$731 \quad p = - \left( \frac{\partial U}{\partial V} \right)_{S, n_i} \quad (11)$$

732 This applies in an unconstrained phase, for which  $\{V, p\}$  is a conjugate pair in the minimal  
733 set of variables, as defined in Appendix 1.1. In a lattice-constraint solid,  $\{V, p\}$  does not  
734 appear in its minimal set, and the thermodynamic pressure is *not* defined. Depending on  
735 the orientation of the chosen plane in such a solid, the perpendicular force per unit area  
736 varies with the orientation and position of the plane. A scalar “pressure” that *can* be  
737 formed is the mean stress—the average of the principal stresses—which varies with position  
738 in a non-hydrostatically-stressed grain. However, this is not an intensive variable; it is not  
739 constant in an equilibrium as scalar intensive variables are (*nh18*, Sect. 3.2).

740 Chemical potential must also be considered differently in unconstrained and  
741 lattice-constraint phases. In unconstrained phases the chemical potentials of all  
742 end-members are defined and are constant in an equilibrium. Within lattice-constraint  
743 solids only the chemical potentials of exchange end-members are defined and constant in an  
744 equilibrium. The chemical potentials of additive end-members are not defined in a  
745 lattice-constraint solid.

746 For a lattice-constraint solid, the stricture of the lattice constraint does not apply on the  
747 grain boundary itself. Lattice points can be created or destroyed there, representing  
748 growth or dissolution of the grain. At grain boundaries, the chemical potentials of all  
749 end-members are defined, the connection to the chemical potentials of the exchange  
750 end-members in the solid being by the interface equilibrium, *nh18*, Sect. 3.7. The chemical  
751 potentials of all the end-members are constant in all grain boundaries and in all  
752 unconstrained phases in an equilibrium. The pressure used in the interface equilibrium is  
753 the negative of the principal stress normal to the grain boundary (for planar and greased  
754 boundaries), e.g. *nh18*, Eq. 22. This pressure varies in a grain boundary between  
755 lattice-constraint solids, but is constant and equal to the thermodynamic pressure with an  
756 unconstrained phase, at equilibrium. For chemical potentials to be constant in grain  
757 boundaries in an equilibrium, the range of pressures in the grain boundaries is constrained  
758 to be small, *nh18*, Sect. 3.7. The quantity “pressure” that is commonly understood to be  
759 reflected in an equilibrium mineral assemblage refers to this narrow range of pressures on  
760 grain boundaries, and not to some average of mean stress within the grains.

761 The creation or destruction of lattice points at a grain boundary is both the mechanism  
762 by which equilibrium stress relations are established at the grain boundaries of  
763 lattice-constraint solids, and that by which the chemical potentials of additive  
764 end-members reach constancy on grain boundaries at equilibrium (as above). Creation or  
765 destruction of lattice points within unconstrained phases is the mechanism by which the  
766 grains reach a state of constant pressure at equilibrium.

#### 767 **Appendix 1.4: Equilibrium relations**

768 Equilibrium defined by energy minimisation leads to equilibrium relations in terms of  
769 chemical potentials corresponding to balanced chemical reactions between the  
770 end-members of phases. In systems containing lattice-constraint solids, minimising an  
771 energy is non-trivial, e.g. Larché & Cahn (1973), Sect. 3b. However in systems containing

772 only unconstrained phases at constant  $p$  and  $\theta$ , the energy to minimise is the Gibbs energy,  
 773 and the minimisation can be done in a straightforward way using Lagrangian multipliers,  
 774 e.g. Smith & Missen (1982). This is a useful exercise as it shows that the chemical  
 775 potentials of components are defined in such systems, and are constant at equilibrium.

776 The Gibbs energy in each phase is written in the usual way as a linear combination of  
 777 the chemical potentials of end-members. Consider an equilibrium involving olivine (ol) and  
 778 orthopyroxene (opx) in FeO–MgO– SiO<sub>2</sub>. A model of the phases is chosen so that the  
 779 end-members of olivine are Fe<sub>2</sub>SiO<sub>4</sub> and Mg<sub>2</sub>SiO<sub>4</sub> and of orthopyroxene are Fe<sub>2</sub>Si<sub>2</sub>O<sub>6</sub> and  
 780 Mg<sub>2</sub>Si<sub>2</sub>O<sub>6</sub>. The Fe–Mg order-disorder in olivine and opx is ignored for simplicity. The  
 781 Gibbs energy in terms of the number of moles of the end-members in an arbitrary amount  
 782 of system is

$$783 \quad G = n_{\text{Fe}_2\text{SiO}_4}^{\text{ol}} \mu_{\text{Fe}_2\text{SiO}_4}^{\text{ol}} + n_{\text{Mg}_2\text{SiO}_4}^{\text{ol}} \mu_{\text{Mg}_2\text{SiO}_4}^{\text{ol}} + n_{\text{Fe}_2\text{Si}_2\text{O}_6}^{\text{opx}} \mu_{\text{Fe}_2\text{Si}_2\text{O}_6}^{\text{opx}} + n_{\text{Mg}_2\text{Si}_2\text{O}_6}^{\text{opx}} \mu_{\text{Mg}_2\text{Si}_2\text{O}_6}^{\text{opx}},$$

784 obtained from  $G$  being additive and also Euler's theorem, Callen (1980), Sect. 3.1. The  
 785 composition of the system, in terms of the number of moles of the components (oxides),  
 786 can be written in terms of the compositions of the end-members

$$787 \quad n_{\text{FeO}} = 2n_{\text{Fe}_2\text{SiO}_4}^{\text{ol}} + 2n_{\text{Fe}_2\text{Si}_2\text{O}_6}^{\text{opx}}$$

$$788 \quad n_{\text{MgO}} = 2n_{\text{Mg}_2\text{SiO}_4}^{\text{ol}} + 2n_{\text{Mg}_2\text{Si}_2\text{O}_6}^{\text{opx}}$$

$$789 \quad n_{\text{SiO}_2} = n_{\text{Fe}_2\text{SiO}_4}^{\text{ol}} + 2n_{\text{Fe}_2\text{Si}_2\text{O}_6}^{\text{opx}} + n_{\text{Mg}_2\text{SiO}_4}^{\text{ol}} + 2n_{\text{Mg}_2\text{Si}_2\text{O}_6}^{\text{opx}}$$

790 To minimise  $G$  at constant composition, the  $G$  is augmented with terms involving the  
 791 Lagrange multipliers of the oxides,  $\lambda_i$ , and these composition identities

$$792 \quad G + \lambda_{\text{FeO}}(n_{\text{FeO}} - 2n_{\text{Fe}_2\text{SiO}_4}^{\text{ol}} - 2n_{\text{Fe}_2\text{Si}_2\text{O}_6}^{\text{opx}})$$

$$793 \quad + \lambda_{\text{MgO}}(n_{\text{MgO}} - 2n_{\text{Mg}_2\text{SiO}_4}^{\text{ol}} - 2n_{\text{Mg}_2\text{Si}_2\text{O}_6}^{\text{opx}})$$

$$794 \quad + \lambda_{\text{SiO}_2}(n_{\text{SiO}_2} - n_{\text{Fe}_2\text{SiO}_4}^{\text{ol}} - 2n_{\text{Fe}_2\text{Si}_2\text{O}_6}^{\text{opx}} - n_{\text{Mg}_2\text{SiO}_4}^{\text{ol}} - 2n_{\text{Mg}_2\text{Si}_2\text{O}_6}^{\text{opx}})$$

795 Minimising, by differentiating with respect to the number of moles of each end-member,  
 796 and setting the results to zero, gives

$$797 \quad \mu_{\text{Fe}_2\text{SiO}_4}^{\text{ol}} = 2\lambda_{\text{FeO}} + \lambda_{\text{SiO}_2}$$

$$798 \quad \mu_{\text{Mg}_2\text{SiO}_4}^{\text{ol}} = 2\lambda_{\text{MgO}} + \lambda_{\text{SiO}_2}$$

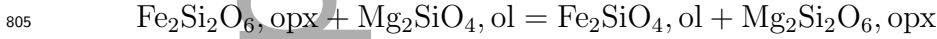
$$799 \quad \mu_{\text{Fe}_2\text{Si}_2\text{O}_6}^{\text{opx}} = 2\lambda_{\text{FeO}} + 2\lambda_{\text{SiO}_2}$$

$$800 \quad \mu_{\text{Mg}_2\text{Si}_2\text{O}_6}^{\text{opx}} = 2\lambda_{\text{MgO}} + 2\lambda_{\text{SiO}_2}$$

801 Eliminating the  $\lambda$  terms from these gives the expected exchange equilibrium relation in  
802 terms of the chemical potentials of the end-members of the phases

$$803 \quad \mu_{\text{Fe}_2\text{Si}_2\text{O}_6}^{\text{opx}} + \mu_{\text{Mg}_2\text{SiO}_4}^{\text{ol}} = \mu_{\text{Fe}_2\text{SiO}_4}^{\text{ol}} + \mu_{\text{Mg}_2\text{Si}_2\text{O}_6}^{\text{opx}}$$

804 which corresponds to the balanced reaction between the end-members



806 In this case there is just one equilibrium relation, but in general there are several, of  
807 number given by the nullspace of the composition matrix of the end-members in the  
808 equilibrium. Equilibrium relations are written generically as  $\Delta\mu = 0$ , with the  $\Delta$  an  
809 operator such that  $\Delta\mu \equiv \sum r_i\mu_i$ , with  $r_i$  reaction coefficients.

810 A significant additional result of the derivations is that the Lagrangian multipliers can  
811 be identified with the chemical potentials of the components (in the above, oxides). It also  
812 implies that each is the same throughout the system at equilibrium, as this property is a  
813 key feature of Lagrangian multipliers in such a derivation (e.g. Larché & Cahn, 1973)

## 814 **Appendix 1.5: Irreversible thermodynamics**

815 The approach followed by, for example Powell *et al.* (2005) and White *et al.* (2008, 2011)  
816 follows that of Korzhinskii (1959) in taking it as self-evident that a local equilibrium  
817 approach, called mosaic equilibrium by Korzhinskii, can be followed. Thus, it is assumed  
818 that equilibrium ideas can be applied on some smaller scale, whereas disequilibrium occurs  
819 on some larger scale.

820 Classical irreversible thermodynamics provides an underpinning for the Korzhinskii  
821 approach, e.g. Kondepudi & Prigogine (1998), Part 4, and Lebon, Jou & Casas-Vázquez  
822 (2008), Ch. 2. Adopting the continuum physics view of considering a system in terms of  
823 particles or material points (e.g. Gurtin *et al.*, 2010, Sect. 5.1), in classical irreversible  
824 thermodynamics, the thermodynamics of each material point is considered precisely as it  
825 would be in equilibrium thermodynamics, that is, with the same minimal set of pairs of  
826 variables for the type of phase, and the same expression for the energies, e.g. (3–4). It is  
827 understood that the material points can interact with each other and therefore their  
828 properties and relative positions within the system may vary with time. With a  
829 dependence on boundary conditions, the behaviour of the system is predicated on the  
830 integral over space of the entropies of the material points, given the constraint of the

831 second law of thermodynamics that the overall entropy must increase (or not change). As  
832 formulated, the entropy constraint leads to equilibration processes that involve linear  
833 combinations of forces and fluxes, with rules that control how the fluxes may be coupled to  
834 forces. In the case of diffusive equilibration at thermal and mechanical equilibrium, the  
835 “forces” are the chemical potential gradients and the fluxes give rise to composition  
836 changes, with the fluxes coupled to all forces. The construction and use of  $\mu$ - $\mu$  diagrams  
837 following the Korzhinski approach is consistent with classical irreversible thermodynamics.

838 Internal equilibria within phases correspond to reactions between end-members such as  
839 between species in a fluid, or for intracrystalline equilibria, e.g.  $2\text{Mg}_{\text{M1}}\text{Fe}_{\text{M2}}\text{Si}_2\text{O}_6 =$   
840  $\text{Mg}_{\text{M1}}\text{Mg}_{\text{M2}}\text{Si}_2\text{O}_6 + \text{Fe}_{\text{M1}}\text{Fe}_{\text{M2}}\text{Si}_2\text{O}_6$  in orthopyroxene. These reactions can be written as  
841  $\Delta\mu = 0$  at equilibrium, as in Appendix 1.4. In classical irreversible thermodynamics, such  
842 internal equilibria, at thermal and mechanical equilibrium, can be written as  $\Delta\mu = A$ ,  
843 where  $A$  is the affinity, e.g. Kondepudi & Prigogine (1998), p103 *et seq.*, following earlier  
844 work of de Donder. The magnitude of  $A$  represents the departure from equilibrium; on  
845 equilibration,  $A = 0$ . It is worthwhile noting that the word, affinity, is used in other ways  
846 in the metamorphic geology literature, all in the context of  $\Delta\mu$  for reactions between  
847 end-members, but in ways that are inconsistent with the original meaning.

848 In the context of over-stepping of simple reactions, with just one reaction between  
849 end-members, introducing a phase not yet present in the assemblage,  $\Delta\mu$  can be thought of  
850 as the integrated driving force for nucleation of the new phase (Hillert 2008, p142).  $\Delta\mu$   
851 then relates to the Gibbs energy difference between the metastable equilibrium, in which  
852 the new phase has not nucleated, and the stable one that includes the new phase.  $\Delta\mu$  is  
853 not an affinity as defined by Kondepudi & Prigogine (1998). A finite value of  $\Delta\mu$  does not  
854 indicate that the system is not in equilibrium, only that the equilibrium is a metastable  
855 one.

856 There is no length-scale involved in  $A$ : for  $A$  the  $\Delta\mu$  considered is “at a point”,  
857 spatially. If  $\Delta\mu$  is used when there is a length-scale involved, when the phases are spatially  
858 separated, then it is critical to understand how the relevant  $\mu$  vary with distance. If the  
859 phases are not in equilibrium with each other, chemical potential gradients will be present.  
860 The resulting  $\Delta\mu$  is not an affinity, and, because of the  $\mu$  gradients implied, is unlikely to  
861 be useful (c.f. Wheeler, 2014).

862 **Figure Caption**

Figure 1: Qualitative Gibbs energy–composition diagram for  $\text{Al}_2\text{O}_3$ - $\text{SiO}_2$  with exaggerated non-stoichiometric phases at fixed pressure and temperature.

Author Manuscript

Gibbs energy

